FIELD TESTS OF TIMBER RAILROAD BRIDGE PILES

A Thesis

by

KENDRA ANN DONOVAN

Submitted to the Office of Graduate Studies of
Texas A&M University
in partial fulfillment of the requirements for the degree of

MASTER OF SCIENCE

December 2004

Major Subject: Civil Engineering

FIELD TESTS OF TIMBER RAILROAD BRIDGE PILES

A Thesis

by

KENDRA ANN DONOVAN

Submitted to Texas A&M University
in partial fulfillment of the requirements
for the degree of

MASTER OF SCIENCE

Approved as to style and content by:

Gary Fry (Chair of Committee)	Terry Kohutek (Member)
Anne Raich (Member)	Paul Roschke (Head of Department)

December 2004

Major Subject: Civil Engineering

ABSTRACT

Field Tests of Timber Railroad Bridge Piles. (December 2004)
Kendra Ann Donovan, B.S., Texas A&M University
Chair of Advisory Committee: Dr. Gary T. Fry

The objective of this thesis is to explore the possibility of a non-destructive method of improving the dependability and economy of timber railroad bridges that have been exposed to environmental and service conditions. With railway companies increasing the load of trains in return for larger profit, maintenance and replacement of timber bridges has risen throughout recent years. Once chosen for its low cost and ease of construction, timber bridges are being replaced by more efficient concrete and steel trestles.

The load path of a passing train through the elements of a bridge pier can be affected for several reasons. One focus of this report is how the load is distributed among the piles or supporting elements.

Through recent research at Texas A&M University (2003), a relationship between the ultimate test load, P_{max}, and the strength parameter, λ, was derived from 33 destructively tested specimens. Piles used in the testing were accumulated from three different locations in the United States and subjected to uniaxial compression along the length of the pile in a steel test frame. Instrumentation along the length of the piles provided data for plots of load versus deflection. Analysis of the plots showed that the tendency of the strength parameter, λ, to predict the ultimate test load was consistent but a computer generated model representing a typical service train revealed significantly lower loads on the piles than those used in the destructive tests. Further analysis of the test specimens at lower load levels led to a service level strength parameter that was derived with levels comparable to typical train loads. Guidelines for the service strength parameter, β, were based upon hypothetical loads from the computer generated model and previous test data. Field testing involved consent from a railroad company to install load cells and string potentiometers on an in-situ timber bridge. While simultaneously taking load and deflection measurements for bridges under the dynamic load of a passing train, the axial stiffness of the piles was determined and used in the calculation of the service level strength parameter, β.

Future research includes removing the piles that were tested in the field and assessing them in the original method of axial compression in the steel test frame. This method can be used universally in the field to examine load path of passing trains and assess the amount of remaining axial strength of in-situ piles without interrupting daily flow and traffic of the railroad bridge. Ultimately, this research could lead to the railroad industry saving money and time due to the quick and convenient installation process.

ACKNOWLEDGEMENTS

I would like to thank the members of my thesis committee, Dr. Terry Kohutek and Dr. Anne Raich, and committee chair, Dr. Gary T. Fry for all of their efforts in completing this research project. In addition, I would like to thank Dick Zimmer of Texas Transportation Institute at Texas A&M University Riverside Campus for all of his expertise needed in the instrumentation and implementation of the project. Furthermore, I would also like to thank Andrew Fawcett, Jeff Perry, and Matt Potter of the Texas Transportation Institute at Texas A&M University for helping out with every aspect in the laboratory. This project would not be possible if it were not for two of my predecessors Brent Bartell and Peter Sculley who paved the way for graduate research studies on this project. The field tests conducted for this research project were completed successfully because of all the hard labor and generosity of Richard Gehle, Dr. Gary Fry, and the many men of Burlington Northern-Santa Fe Railroad Company. For all of my hard work, there have always been two people who have supported me through every moment and for that, I am forever thankful to my parents. The completion of my collegiate work marks the beginning of my engineering career, and I cannot wait to share the new experiences with all of my family, friends, and mentors who have impacted my life.

TABLE OF CONTENTS

LIST OF FIGURES

LIST OF TABLES

CHAPTER I
INTRODUCTION

1.1 BACKGROUND

As with all other modes of surface transportation, bridges are a crucial element of the physical infrastructure of railroads. Made primarily from steel, concrete, wood or a combination of these materials, many railroad bridges in North America have been in service for over 75 years. However, recent changes in railway operations have placed more physical demand on railroad bridges in North America. To improve profitability, many Class-I railway companies have eliminated redundant routes thereby concentrating traffic to main lines. In addition, maximum allowable payloads have increased. The two primary mechanical consequences of these operational changes are increased amplitude and increased frequency of applied loads that must be resisted by structural components in bridges.

The profit realized by these operational changes is partly offset by the increased cost of maintaining the bridges subjected to the more demanding loading. Railway industry surveys have indicated that when operational demands increase, timber bridges require a disproportionately larger inspection and maintenance investment as compared to steel or concrete systems (Uppal and Otter 1998). As a result, it is common to replace timber bridges with steel or concrete when budgets allow for bridge renewals. This is a gradual process, however, because timber comprises roughly one-third of the total length of North American railroad bridge spans (AAR 2001). Timber piling is even more common than timber spans, because it is sometimes used to support steel and even concrete spans. Replacing all of the timber spans and timber piling in an aggressive program of renewal would be prohibitively expensive, likely more than offsetting any profit to be gained by operational changes. Clearly there is a need for an accurate and precise assessment of timber bridge component performance. This study focuses on means of assessing the behavior of timber piling in railroad bridges.

This thesis follows the style of *Journal of Structural Engineering.*

A typical cross section and lateral view of a timber bridge are shown in Figures 1.1 and 1.2. The load from train axles applied directly to the rails are distributed to the nearest ties which are typically placed 19 to 20 inches apart transversely along stringers (AREA 1997). The stringers are large, rectangular beam-like elements spanning in groups of 4 or 5 per chord between adjacent bent caps where the load is collected and allocated among the supporting piles. "Each bent has four or more vertical members, either wood posts resting on concrete footings of wood pilings driven into the ground to serve both as foundation and vertical member of the bent. Timber piles are column-like elements that transfer vertical and lateral loads into the soil. Usually, the outer pile on each side is battered so that the bent will be able to resist lateral load" (Stalnaker 1997). For the purposes of this report, the foundation beneath all the piles is assumed rigid and sufficient enough to support the self-weight of the timber bridge structure and train loads.

Decay of timber piles is a result of moisture conditions and exacerbated by biological insects. Throughout years of service, piles infected with decay lose stiffness and the ability to participate in efficient load sharing among adjacent piles. Current investigations of decay in timber piles involve removing portions of the cross-section through bored holes and assessing the amount of dead wood in that particular section. However, individual holes at sparse intervals along the pile does not accurately assess the true damage hidden throughout the pile.

1.2 OBJECTIVE

The aim of this project is to assess load distribution among timber piles while allowing the industry to continue serving customer demands. With basic instrumentation, railroad engineers and designers could have a better understanding of how the bridge structure is operating from an internal vantage point in order to maintain and repair it efficiently. From the basic mechanical perspective of the timber bridge structure, one might hypothesize that all of the piles under the bent cap experience the same load, but an important aspect of this project focuses on how the piles participate in the load resistance path. Previous destructive tests and analysis revealed a pile strength parameter, λ, that

estimated the residual strength or ultimate capacity of the pile. “Direct-stress fatigue tests generally are considered to be most applicable for wood-base materials, because the uniformity of stress produced across the section of the specimen allows the data obtained to be used to better advantage in full-sized structures. With a constantly increasing load, it is easily possible to test specimens to destruction and such a procedure has appeared for testing wood and glue-wood constructions” (Lewis 1946). However, by using non-destructive testing methods, this project includes previous research methods combined with new analysis to correlate residual strength and service loads applied to timber piles. The integrity of the piles is directly affected by environmental and service conditions. For instance, the possibility of decay in wood increases with the occurrence of moisture cycles such as the rise and fall of flood waters. The stiffer piles should expect to resist more load while the piles that account for a comparatively smaller load are less stiff and most likely suffer from more decay. If successful, the methodology developed in this project should improve both the safety and reliability of operations over timber railroad bridges.

1.3 DETERIORATION OF PILES

Both the effects of cyclical weathering and mechanical wear catalyze the softening of wood with the presence of decay in the timber structure. Fungi that attack wood species must have air and moisture in order to survive. If timber species are kept at low temperatures and completely dry, then it could remain immune for more than a hundred years (Capozzoli 1996). In a similar manner, piles that are submerged under water where contact with the air is limited could also last for similar time periods. Piles located in areas where water is constantly changing depth suffer from the most decay at the water surface due to the wet and dry cycles. Using preserving treatments on timber increases the wood’s natural durability because of the toxic effects on insects, fungi, and marine borers. “Unlike many materials, wood is resistant to mild chemicals and insulates against electricity and heat. Indeed, the air trapped inside its cellular structure makes timber the best thermal insulator of all known building materials” (Wilkinson 1979). Even though wood provide an excellent source of strength in structures, it is susceptible to fire, insects, fungi, and marine borers (Cook 1987). There are three axes in characterizing wood structures: axial, radial, and tangential. Each direction shrinks and swells at different rates and also resists load at varying capacities. The

density of a timber can also affect the strength because of the amount of wood available to be decayed. A higher density timber contains more wood material, and therefore it can resist a larger load than a less dense timber of the same size.

> Heartwood has the same strength as sapwood but has greater natural durability of the toxic compounds deposited in the cells during its formation and also because of its lower permeability to water and oxygen. Indeed, the poor natural resistance of sapwood is particularly acute immediately after the tree has been felled when the moisture content is high and contains high levels of starch and soluble carbohydrates. In this condition the sapwood zone is susceptible to invasion by staining fungi, moulds and insects, and if left untreated with an appropriate preservative chemical or rapidly dried, the wood will deteriorate quickly (Eaton 1993).

Typically, the tip end of the pile which is driven into the ground suffers from more decay than the opposing end that is connected to the bent cap. The wet and dry cycles at ground level initiate and sustain the processes of biological decay. Nonetheless, the state of current timber railroad bridges in the United States is proof of their longevity and ability to withstand undesirable environmental conditions (Ross 2002).

In all timber species, visual inspections for defects that are a detriment to the strength include knots, slope of grain, rate of growth, fissures, bark pockets, and distortion, but the integrity of timber strength is mostly dependent on density, moisture content, and duration of load. "The timber preserving industry began in England and provided considerable quantities of long-lasting sleepers and poles for the growing railway and telegraph systems" (Wilkinson 1979). While protecting against splitting and weathering, creosote also makes the timbers insoluble to water and resistant to leaching. Treatment of timber can be accomplished through several methods of application including empty-cell pregnation and injectors where wood is impregnated with preservative under high pressure on top of air trapped within the wood. Creosote injected timber piles have been simplified over the past years by injecting the preservative at high pressure through a gun while simultaneously maintaining the pressure within the wood (Cartwright 1950).

1.4 PREVIOUS TESTING AT TEXAS A&M UNIVERSITY

In 2001-2002, destructive tests were performed on 33 creosote treated timber piles gathered from across the United States. Upon arrival, visual inspections for knots, exterior decay, splitting, and other defects were completed to further understand the modes of failure on the piles of varying size and origin. Pretest procedures included measuring pile dimensions such as length and circumference along the length of the specimen in order to find the least diameter (see Table 1.1). The condition of the piles were photographed and catalogued for comparison purposes during the analysis phase of the project. The removal of all metal attachments served as a safety precaution during the physical testing of the piles, but also made loading the piles into the testing apparatus more concise without the interference of metal pieces such as the drift pin. The piles were subjected to a constantly increasing, axial compressive load in a custom frame until the ultimate load was reached. "The frame consisted of three W24x124 members, 58 feet in length bolted through the webs to the arms of a fixed headstock and a fixed tailstock at varying lengths" (Sculley 2003). The three W-shapes were designed in a Y-shape at equal angles from each other. A hydraulic jack at one end of the frame provided the load that traveled through the pile and into a fixed headstock with a load cell at the opposite end supporting the pile until it failed under the load. Three linear variable displacement transducers (LVDTs) simultaneously captured the average deflection of the pile along the three W-shapes on the frame (see Figure 1.3). The modes of failure included one or more of the following: longitudinal splitting along the length of the pile, localized barreling of the cross section, lateral buckling, and manual termination due to failure to sustain load (Sculley 2003).

The results from the testing of specimen A7 are shown in Figure 1.4 on a plot of axial load versus deflection. A similar graph was prepared for each pile, and the slope, $(EA/L)_{test}$, of the linear portion was used in the derivation of the strength parameter, λ shown in Figure 1.5. The pile strength parameter in Equation (1.2) is a slight variation of the Euler buckling equation (Equation 1.1) and accounts for the reduction in axial stiffness due to decay as well as the member slenderness (Sculley 2003):

$$P_{cr} = (p^2/16)*(EA/L)*(d^2/L) \quad (1.1)$$

$$\lambda = (EA/L)_{test}*(d^2/L) \quad (1.2)$$

where d and L are the least diameter and length of the pile, respectively. Finally, the data from the test specimens was analyzed using a mean regression line:

$$P_{max\_95\%} = 2.04\lambda^{(.673)} \quad (1.3)$$

$$R^2 = .876 \quad (1.4)$$

The analysis of a 95 percent lower confidence limit shown in Figure 1.5 resulted in the following equation:

$$P_{max\_95\%} = 1.15\lambda^{(.673)} \quad (1.5)$$

$$R^2 = .876 \quad (1.6)$$

Previous testing concluded that the high coefficient of correlation obtained from the least squares regression analysis suggests a strong relationship between the pile strength parameter and pile capacity. By using the mean regression results, the ultimate load could be estimated for a given pile. However, computer analysis of the effects of a typical train crossing a two span timber bridge (see Figure 1.6) revealed significantly lower loads in the piles than had been used to derive the strength parameter as it appears in Figure 1.5. Therefore, this project in addition to examining the load distribution among piles, also inspected the correlation of ultimate capacity with pile response under service load conditions.

After failure in the test frame, the piles were destructively sampled for decay by making slices at one-foot intervals along the length of the specimen. This particular procedure captured the actual decay on the cross sections throughout the length of the pile to scrutinize the state of wood that was not visible from the exterior. Decayed areas of wood were considered ineffective, and therefore not included in the calculation of area for each cross section. The ideal area was calculated from the circumferential measurements at both ends of the pile during the initial inspection. However, in order to find the actual area of good wood, photographs were taken of each cross section and covered with a piece of transparent grid paper. By comparing the number of grid spaces filled with decayed wood versus the number occupied by the total cross section, the actual amount of good wood participating in the resistance of load was computed. In fact, these results confirmed theories of the tip ends of the specimens suffering from more damage than the ends further from the ground. The purpose of characterizing and grouping piles by level of decay is to find the point where the decay causes potential danger to the structure (Donovan and Fry 2002).

CHAPTER II
PROCEDURES

2.1 DATA ACQUISITION SYSTEM

Similar to the custom steel frame utilized in the previous research procedures, equipment for the current testing procedures was also designed and built at Texas A&M University for this particular application (see Figure 2.1). The unique data acquisition system provided the basis for collecting information from 32 instruments. A variety of devices such as strain gage and feed through modules were necessary for the instruments to interact with LabView. National Instrument's LabView is the graphical development environment for creating flexible and scalable test, measurement, and control applications rapidly and at minimal cost. With LabView, users interface with real-world signals, analyze data for meaningful information, and share results and applications. The LabView program includes wiring tools and a user-interface that allows the instrumentation in this project to be represented electronically. A laptop computer allowed for all of the input collected from the field to be stored and converted from voltage into practical output placed directly into Excel files. Approximately 1,500 feet of cable supplied power to the instruments from a portable generator on site and provided a path for the LabView program to collect data.

2.2 INSTRUMENTS

The equipment used in this project reflects the need to assess the reaction of a pier due to a train load without damaging elements of the timber bridge structure. Two data acquisition cards offered 16 channels each or a total maximum of 32 channels of input. The 16-bit cards were plugged into the laptop and connected to a collection of instruments or devices. Device 1 was labeled with channels 0 through 15 containing a set of 16 string potentiometers with 4 inch maximum available length. The maximum voltage over the 4 inch length of cable was 10 volts. Device 2 contained 2 more string potentiometers and 12 load cells with 30 kip capacity. Strain gages amplified the output voltage of each load cell by 100 in order to read all of the instruments on similar magnitudes of power. The two string potentiometers on Device 2 were routed into feed through modules to take advantage of unoccupied channels. Two channels on Device 2 remained vacant but were kept available

for back up instruments or additional piles in a pier that needed to be instrumented. As the instruments experienced voltage changes, LabView acquired the data and transferred it into usable data such as load and deflection measurements with units of kips and inches, respectively. For instance, the string potentiometers experienced a positive voltage change as the cable was pulled out and a negative reaction when the cable was released simulating compression behavior. Calibration factors that were assigned to load cells by the manufacturer were confirmed under laboratory conditions while the string potentiometers were also calibrated to confirm a linear relationship. Each pile simultaneously used three string potentiometers and two load cells to acquire load and deflection as a result of the train load. Simple ratcheting straps placed at the ground surface and top of the pile provide mounting brackets for the string potentiometers. The string potentiometers were attached to stiff wood boards and placed underneath the ratchet strap through angle brackets. Fishing line spanning between the ratchet straps on each pile provided enough tension on the string potentiometers to record the deflection along the length of the pile due to the train load. Two steel plates surrounding the load cells (see Figure 2.2) ensured that the timber piles were not damaged by load cells puncturing the wood as well as provided stiffness to transfer the train load from the bent caps into the piles.

2.3 CONDITIONS OF FIELD TESTING

A good bridge candidate for this project included timber piles that have been subjected to typical environmental conditions or fatigue damage over its lifetime. Burlington Northern-Santa Fe Railway Company provided the timber bridge located in Houston, Texas where the environment tends to be hot throughout the year with mild winter months. Rain and humidity are two environmental detriments that commonly plague this geographical area. One example of current damage to this bridge is a horizontal shear crack (see Figure 2.4) due to an overload in shear capacity which represents the increase in load demands through recent years. This bridge which is located on line 492 at station 58:81 was currently undergoing construction to convert the southern pine timber bridge structure into one of steel and prestressted concrete at the time of testing. Steel W-shapes were driven into the ground next to the timber piles and once the piles are removed, prestressed concrete will span across the new piles. Due to the condition of the bridge, a maximum speed limit of 20 miles per

hour was previously imposed on crossing trains. The bridge was located above a small bayou where the piles instrumented were located well above water level in a bed of rocks. The pier used in this experiment contained six timber piles with a seventh timber post. Drift pins connecting the outer piles to the bent cap were used to stabilize the overall structure during loading.

2.4 CURRENT FIELD TESTING PROCEDURES

Abiding by the regulations of Burlington Northern-Santa Fe Railway Company, every member of the research team completed a safety awareness program before conducting field experimentations. Basic guidelines for railroad procedures included reviewing safety equipment and etiquette around the railway. Upon arriving on the bridge site, the timber piles were photographed and tagged in regards to their in-situ location relative to the North-South direction of the train tracks. The location of the piles underneath the bent cap was necessary for the analysis of the load sharing phenomena between the piles. Since the timber piles will be removed from service and shipped to Texas A&M University for future testing, the identification markings were made of a high strength fluorescent paint in order to withstand harsh conditions under transportation. Figure 2.4 shows the tagged piles under the bent cap where the identification process included marking each of the piles with numbers from one to seven referring to their position under the bent cap. For instance, the far left pile facing the North direction was labeled with a "1" and the right was labeled with "7". Pretesting procedures also include measuring pile dimensions such as circumference and length. Since piles are tapered from one end and timber is a natural product with imperfections, the term circumference for all purposes in this project is the least circumference measured along the pile length. From the circumference, the least diameter can then be easily calculated.

String potentiometer mounting brackets were made from 6" x 6" blocks of stiff wood and 4" angle brackets that allowed them to lay flush against the circumference of the piles. Three string potentiometers were fastened to the bottom of each pile by a ratcheting strap (see Figure 2.5). Eye bolts connected to small angle brackets hooked underneath ratchet straps were used as anchors at the top end of the pile (see Figure 2.6) while fishing line was connected at both ends. Because the timber piles undergo compression under train loads, the

cables on the string potentiometers were initially pulled out in tension so that the cable would remain tight under axial compression of the piles. The pile length for derivation of the strength parameter, λ is defined as the clear distance from the bottom of the bent cap to the ground surface between the ratchet straps. There was a 2.5 inch shim located above the bent cap to keep the tracks in a horizontal position. In order for the load cells to be placed above the piles, the entire bent cap needed to be raised two inches while still maintaining the safety standards set by the railroad industry. To accomplish this task, Burlington Northern-Santa Fe Railway Company provided two cranes with the larger of the two weighing approximately 298 kips. As one crane raised the chords of stringers and removed the shims to make room for the steel bearing plates, the other crane lifted the bent cap off of the piles. It was only at this point that the load cell plates could be installed above the piles (see Figure 2.7). The steel bearing plates had a center cutout that accounted for the location of the drift pin in the center of the pile as shown in Figure 2.2. The load cell plates were secured in place around the drift pin by machined bolts around the circumference of the plates. To keep the bent cap stable during this experiment, the load cells were arranged perpendicular to the length of the bent cap (see Figure 2.8) which allowed for negligible moment over the piles. Unfortunately, Pile 7 was obstructed by diagonal bracing and therefore was not suitable for instrumentation during the test. Instead, sufficient shims were placed above the pile to maintain contact with the bottom of the bent cap. Pile 5 was actually a post with square dimensions and provided an adequate surface for only 2 string potentiometers. Piles 1 through 4 along with Pile 6 were all instrumented with two load cells and three string potentiometers.

Once the instrumentation was secured, the speed of the approaching train was limited 10 miles per hour to ensure the structural integrity of the bridge and its surroundings. This type of instrumentation of a bridge is not typical and consequentially, the speed limit was strictly enforced. The trains used in this field test were a mixture of classes and contained different cargo. A typical setup for this type of train includes several engines and a variety in the lengths and types of cars. The advantage of using this lightweight instrumentation was that once the train passed the bridge, the equipment was immediately removed and the pile was restored to its original condition.

2.5 LOAD APPLICATIONS

The field testing process was unpredictable because of the constantly changing schedule and coordination routine between railway companies. Researchers were allotted time slots in between scheduled arrivals of passing trains. The first break allowed for enough time to lift the bent cap and install the load cells before the track had to be cleared once again. In this report, Crane A was the first load on the instrumented bent cap as the crane lowered the chords into position and passed over the bent during its departure. Arrival of Train A came shortly after the load cells had been placed above all of the piles and allowed for only enough time to instrument three string potentiometers on Pile 3. Piles 3, 4, 5, and 6 were then fully instrumented with load cells and string potentiometers that captured the reactions from Train B. After all of the piles had been completely instrumented, Train C passed over the bridge. However, due to a slight problem with the power source, the data from Train C was insufficient. The final test on the bridge was Crane B lifting the bent cap in order to remove the load cell plates and replace the shims restoring the bridge the bent to pretest state. Although the cases of Crane A and Crane B involved load reactions from a 298 kip crane, the total load was distributed across the piers decreasing the load directly applied to the instrumented pier.

CHAPTER III
RESULTS AND ANALYSIS

3.1 RESULTS FROM FIELD TESTING

Plots of load versus time for each of the piles reaction to Crane B are shown in figures 3.1 through 3.6. The total load from the crane is unknown because Pile 7 was not instrumented, but Figure 3.7 represents the combined load from Piles 1 through 6. In the case of train loading, the front as well as the rear axles of each car that passed the pier resulted in a sudden reaction of increase load in the piles. There was not any information available from Burlington Northern-Santa Fe Railway Company about the class of cargo inside the cars, but the higher peaks in the plots probably represent the heavier or fully loaded cars while the lower peaks most likely represent the empty cars (see Figure 3.8). Located on the outermost edge under the bent cap, Pile 1 sustained a very small load compared to the piles within the distance between the chords of stringers. Results of load distribution for each pile are shown in Figure 3.9.

3.2 ESTIMATING RESIDUAL STRENGTH IN TEST SPECIMENS

During installation, the piles are typically driven into the ground where the capacity depends more upon the soil than timber bearing capacity. Typically, the loads applied to the piles during the driving process will exceed any other loads expected during the life cycle of the timber pile. Destructive tests revealed that piles of similar species failed at a range of compressive loads (see Table 1.1). The largest failure load, P_{max} was 718 kips. The previous field testing in this project used a higher, linear portion of load-deflection plots correlating the λ values with the ultimate strength capacities. However, the computer model representing a typical train load passing over a continuous span bridge revealed lower service loads. The model shown in Figure 1.6 shows that the maximum estimated reaction in the bent cap is 193 kips or approximately 33 kips per pile assuming a 6-bent configuration. A similar linear regression analysis was performed on the regions of the load-deflection plots where the loads were comparable to the hypothetical service loads. For instance, the linear region of Pile A7 in previous analysis is shown in Figure 1.4, but the region selected for emphasis in this project is shown in Figure 3.10. This particular region was chosen because

of the comparable magnitudes of the computer-generated train loads. Therefore, data from 33 piles tested in 2001 at Texas A&M University was reevaluated with the following guidelines for choosing the portions of the slope that were applicable to the service strength parameter β:

- The linear trend line must be applied between 0 and 40 kips.
- Correlation of the trend line should be at least $R^2 = .70$.
- The maximum value of β should be 1327.8 k.
- The minimum value of β should be at least 23.5 k.
- The slope of the linear regression must be positive.
- The smallest slope should be used when there are multiple peaks to ensure conservative estimation of the ultimate capacity.

Extrapolation outside of these boundaries is not practical until further testing has been completed.

The results from the service strength parameter analysis are shown in Figure 3.11 with logarithmic axes due to the linear plot showing a power law regression. The X-axis represents the strength parameter, β for the service loads and the Y-axis is the failure load of the piles, P_{max}. By a least squares fit estimation, the equation of the mean regression line and coefficient of correlation are:

$$P_{max\_50\%} = 1.1553\beta^{(.8869)} \quad (2.1)$$

$$R^2 = .6802 \quad (2.2)$$

where P_{max} is the ultimate strength of the pile for a given value of the strength parameter, β. The equation of the 95 percent lower confidence limit is shown in Figure 2.2 as well and given as:

$$P_{max\_95\%} = .4625\beta^{(.8869)} \quad (2.3)$$

$$R^2 = .6802 \quad (2.4)$$

Data from all of the piles used in the field experiment was used to create load-deflection plots similar to those used in previous analysis. The slope of the linear portion, $(EA/L)_{test}$, and the quantity (d^2/L) were multiplied to arrive at the strength parameter, β for individual piles. From this analysis and Equation (2.3), the ultimate loads for the piles were estimated according to the service conditions in Table 3.1.

3.3 DISCUSSION

The ideal mechanical theory of equal load distribution between the piles under the bent cap was disproved in this field test. Pile 1 was located outside the chord of stringers and did not play a major role in resisting the load for any case. Piles 2, 3, 4, and 6 resisted similar amounts of load (see Figure 3.7). Compared to loads experienced in the other piles, the post did not participate as much as the piles in resisting the load. In some cases the piles accounted for more than six times as much load in the post. One reason that the post may not have participated as much as the piles is because of its close proximity to the adjacent piles. The average distance among piles was more than one foot, but the post barely cleared 6 inches between the flanking piles. Perhaps if there was more distance between the post and its neighboring piles, the load would have increased.

Applications of the load path results could play an important role in routine scheduled maintenance. By simply knowing where the load travels, adjustments can be made to distances between the piles and bent cap. Shimming is a common practice in the field, and yet it is not an exact science. When the shimming is too deep, the load path may be interrupted and biased towards certain supporting piles. In the same manner, piles that do not have adequate shimming and lack proper contact with the bent cap will not receive a proportionate amount of the load. Axial stiffness in every timber pile will inherently be different because of the natural imperfections in wood. Nonetheless, an opportunity is presented with these results as they could provide a method balancing the load equally among the piles. A program that uses the reactions in each pile from the field tests could certainly be written to design the proper height between piles and bent caps enabling equilateral load distribution among the piles. Although the bent cap itself was not analyzed in this project, the flexural rigidity of the bent cap is another important factor in determining how the load is allocated to the piles and perhaps will be studied in further testing.

The derivation of the strength parameter in previous and current research has been based on circular timber pile shapes. However, Pile 5 in the test was actually a square post. In order to use the field results in addition with the strength parameter, the area of the square cross section was equated to the formula for the area of a circle to find an equivalent diameter. The strength parameter, β, should be used to estimate the load when the

appropriate level of stiffness, $(EA/L)_{test}$ has been achieved. The coefficient of correlation for β slightly decreased from the results using destructive tests revealing that as the loads applied to the piles increase, the reliability of the strength parameter increases. If the applied load is too small or minimal level of stiffness is not achieved, then the ultimate capacity will be underestimated yielding a conservative estimate. The axial stiffness, $(AE/L)_{test}$ was measured over the entire distance of the piles, but as previous decay analysis revealed, there were localized areas of decay failure. As the natural taper changes throughout the length of the pile, the value (AE) changes accordingly which prevents the ability to quantify the stiffness of the entire pile. One recommendation that has been made in the past is to use smaller lengths along the pile to account for the decay variation. This would require the use more accurate equipment and installation time for each bridge.

One debatable aspect of this project is the instrumentation of the string potentiometers. The string potentiometers were reconditioned from the 1960's and even though they performed well in the laboratory environment, the heat and humidity during the field test may have played a role in their misbehavior. The resolution from the string potentiometers allowed the devices to read displacement increments up to $^{1}/_{1000}$ of an inch. However, the deflection results in the field tests continuously jumped between the range of the string potentiometer resolution while simultaneously attempting to record movement in the piles. From plots of deflection versus time (see Figure 3.12), it seems as though many of the coils inside the string potentiometers were not strong enough or the heat prohibited them from pulling the fishing line back to its initial position after each load cycle. The corresponding plot of load versus time for Pile 6 in Figure 3.6 shows that the load decreases around 57 seconds, but the deflection only seems to continually increase. Another reason to revisit the results is that the fishing line used to cover the length of the pile needed to be in perfect balance with the coil inside the string potentiometers and several cases appear as if the fishing line was pulled too tight. In further field tests, a stiffer connector should be used with instrumentation that will not be affected by the environmental conditions. The piles used in this test were fairly short and did not deflect as much as longer specimens. An interesting addition to this project would be the testing of longer timber piles to compare how the deflections compare to these results.

3.4 FUTURE WORK

This project included the testing of a single group of timber piles in a bridge, and with a larger sampling of specimens available in the future, the relationship of pile load can be further examined. The pile is just one of the elements in the bridge structure that transfers load and as more methods of instrumenting the bridges are created, the more opportunities there will be to sustain longer bridge life spans. Even though this methodology presented a relationship between ultimate capacity and service loads, variation in bridge characteristics such as span length and type of train need to be explored further before conclusive results can be attained. The piles tested in bridge located in Houston, Texas will be transported to Texas A&M University in the next year for destructive tests in the same steel frame as in previous tests. It is only after the destructive tests that the strength parameter β can be proven. Using the strength parameter and the hypothesis of this project, the expectation is that the timber piles should reach or exceed the predicted P_{max} load calculated with the strength parameter. If the goals of this research are achieved, the use of non-destructive test methods will be implemented by the railroad industries and receive more acknowledgements and interest by research institutions across the United States.

CHAPTER IV
CONCLUSIONS

4.1 CONCLUSIONS

After analyzing data from the laboratory along with full-scale tests of in-situ timber railroad bridge piles, the following conclusions were made:

- The largest load as a result from a passing train experienced by a pile was 35 k.
- The smallest load as a result from a passing train experienced by a pile was 3.7 k.
- The piles underneath the bent caps do not experience equal loads, but actually distribute the load from the bent cap according to the stiffness of the piles where the stiffer piles tend to resist larger loads.
- Piles between the chords of stringers experienced more load than the outer piles underneath the bent cap.
- The high coefficient of correlation between the service loads and ultimate capacity least squares regression analysis suggests a valid relationship.
- Ultimate strength parameter, λ, corresponded to a slightly higher coefficient of correlation leading to a stronger relationship than the service strength parameter, β (Ang and Tang 1975).
- The pile stiffness, $(EA/L)_{test}$, is directly related to the ultimate strength of the piles.
- The largest deflection due to a train or crane load was .029 inches in Pile 5 due to Crane B.
- Although the expected loads in the piles from the computer generated were confirmed by the field tests, the relationship between pile location under the bent cap and load should be explored further before using this method in the field.
- Even though the string potentiometers were capable of precise measurements in laboratory conditions, they failed to perform accurately in the field.

REFERENCES

AAR (2001). "Fatigue Strength of Douglas Fir Railroad Bridge Stringers." *Transportation Technology Center, Report No. R-953,* Association of American Railroads, Pueblo, CO.

Ang, H-S. and W.H. Tang (1975). *Probability Concepts in Engineering Planning and Design.* John Wiley & Sons, New York.

AREA (1997). *Manual for Railway Engineering Vol. 2.* American Railway Engineering Association, Washington, DC.

Capozzoli, L. J. (1996). "Current Status of Timber Foundation Piles." *Wood Preserving News,* 44 (11), 11-13.

Cartwright, K.G. and W. P. K. Findlay (1950). *Decay of Timber and Its Preservation.* Chemical Publishing Co., Inc. New York.

Cook, R. J. (1987). *The Beauty of Railroad Bridges.* Golden West Books, San Marino, CA.

Donovan, K. A. and G. T. Fry. (2002). "Testing Timber Piles from Railroad Bridges." *Research Report*. Texas A&M University, College Station.

Eaton, R. and M. D. Hale. (1993). *Wood: Decay, Pests, and Protection*, 1st Ed. Chapman and Hall, London, UK.

Lewis, W. C. (1946). "Fatigue of Wood and Glued-wood Construction." *Proceedings of the American Society for Testing Materials,* Chicago, IL., 53-54.

Ross, P. (2002). *Appraisal and Repair of Timber Structures.* Thomas Telford Publishing, London.

Sculley, P. J. (2003). "Determination of a Strength Parameter for In-situ Evaluation of Timber Railroad Bridge Piles Subject to Decay and Fatigue Damage Accumulation." *M.S. Thesis,* Texas A&M University, College Station.

Stalnaker, J. J. and E. C. Harris. (1997). *Structural Design in Wood, 2nd Ed*., Chapman and Hall, New York.

Uppal, A. S., and D. E. Otter. (1998). "Methodologies for Strengthening and Extending Life of Timber Railroad Bridges." Association of American Railroads, *Transportation Technology center, Report No. R-922,* Pueblo, CO.

Wilkinson, J. (1979). *Industrial Timber Preservation, 1st Ed.* Associated Business Press, London, UK.

APPENDIX A
FIGURES

Fig 1.1 Cross section of piles underneath typical bridge bent cap

Fig 1.2 Lateral view of piles

Fig. 1.3 Steel frame used in previous destructive tests

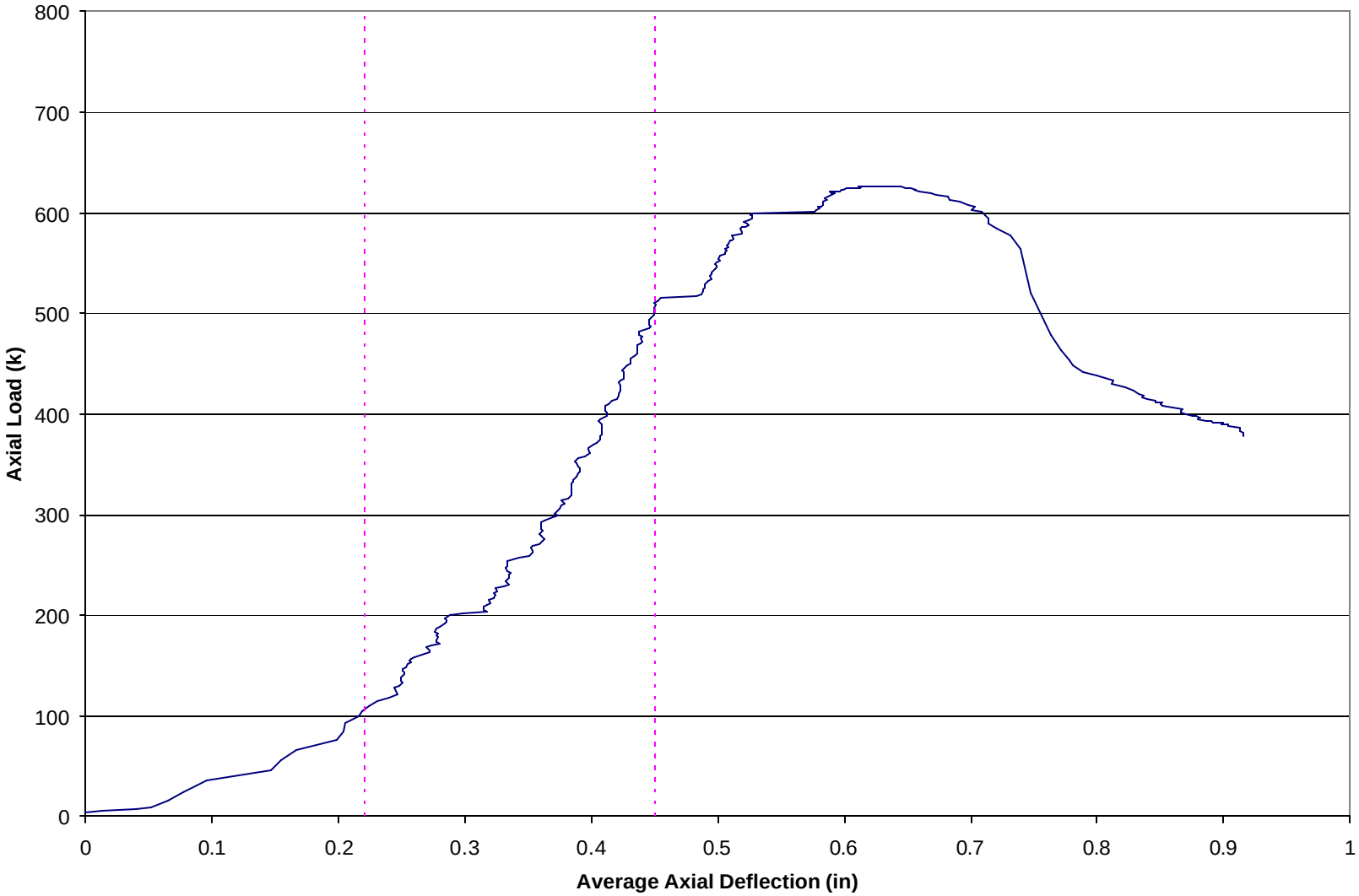

Fig. 1.4 Linear portion of the plot of applied load vs. average axial deflection for specimen A7 used in derivation of strength parameter λ

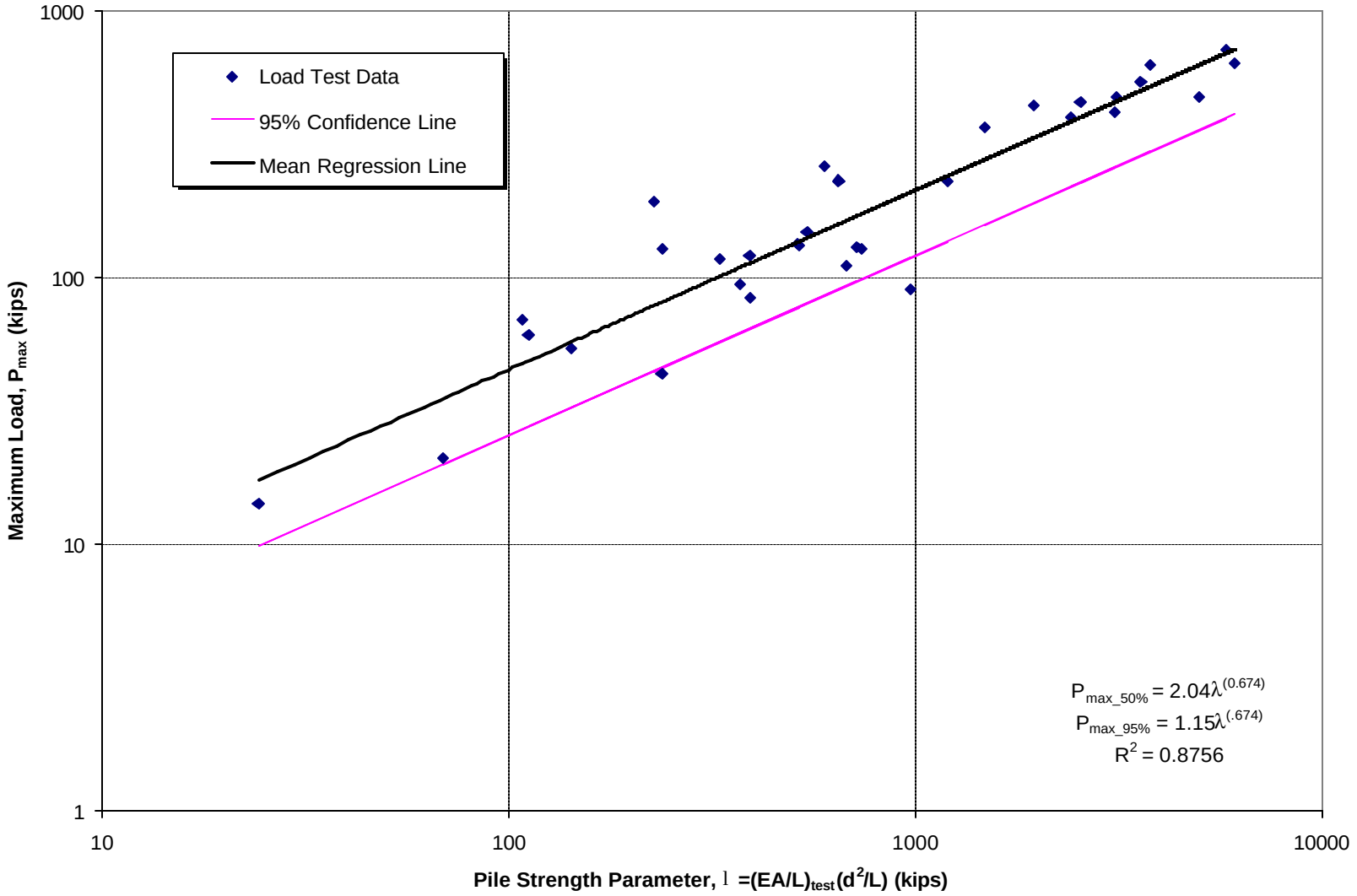

Fig. 1.5 Ultimate load vs. pile strength parameter, λ

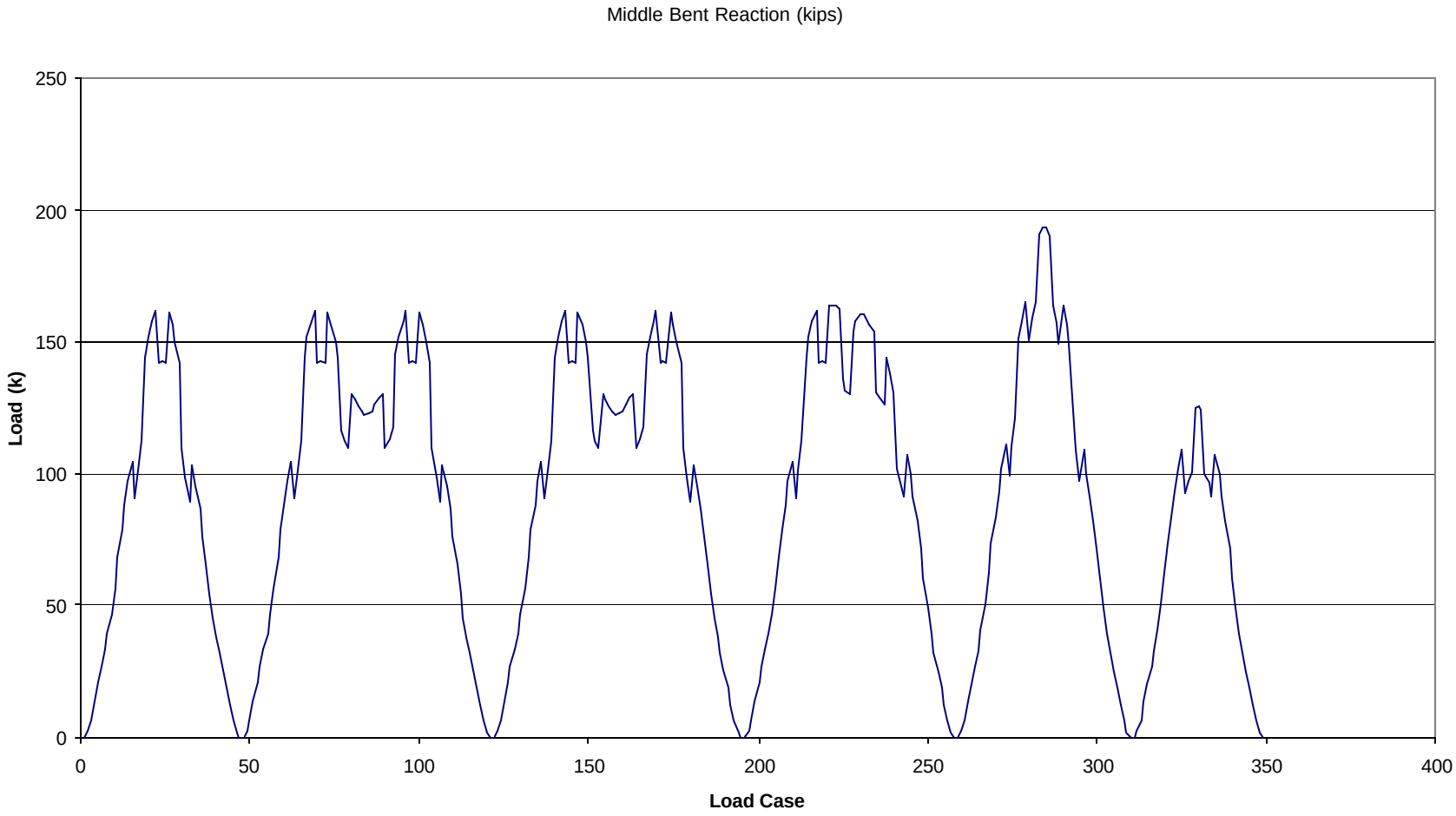

Fig. 1.6 Expected load from computer-generated model of a typical class A train

Fig. 2.1 Data acquisition system

Fig. 2.2 Photograph of load cells in steel bearing plates

Fig. 2.3 Photograph of horizontal shear crack present in stringer

Fig. 2.4 Photograph of piles with identification labels

Fig. 2.5 Photograph of string pots installed on pile near the ground surface

Fig. 2.6 Photograph of eye bolt anchor underneath bent cap

Fig. 2.7 Photograph of load cell installation with crane

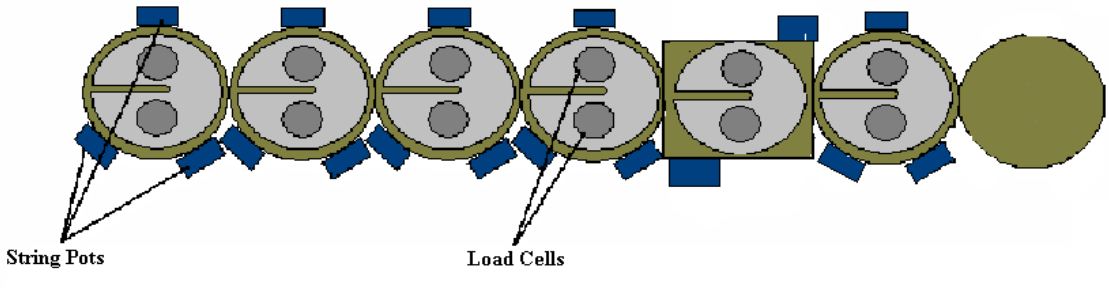

Fig. 2.8 Plan view of load cells and string pot arrangement beneath bent cap

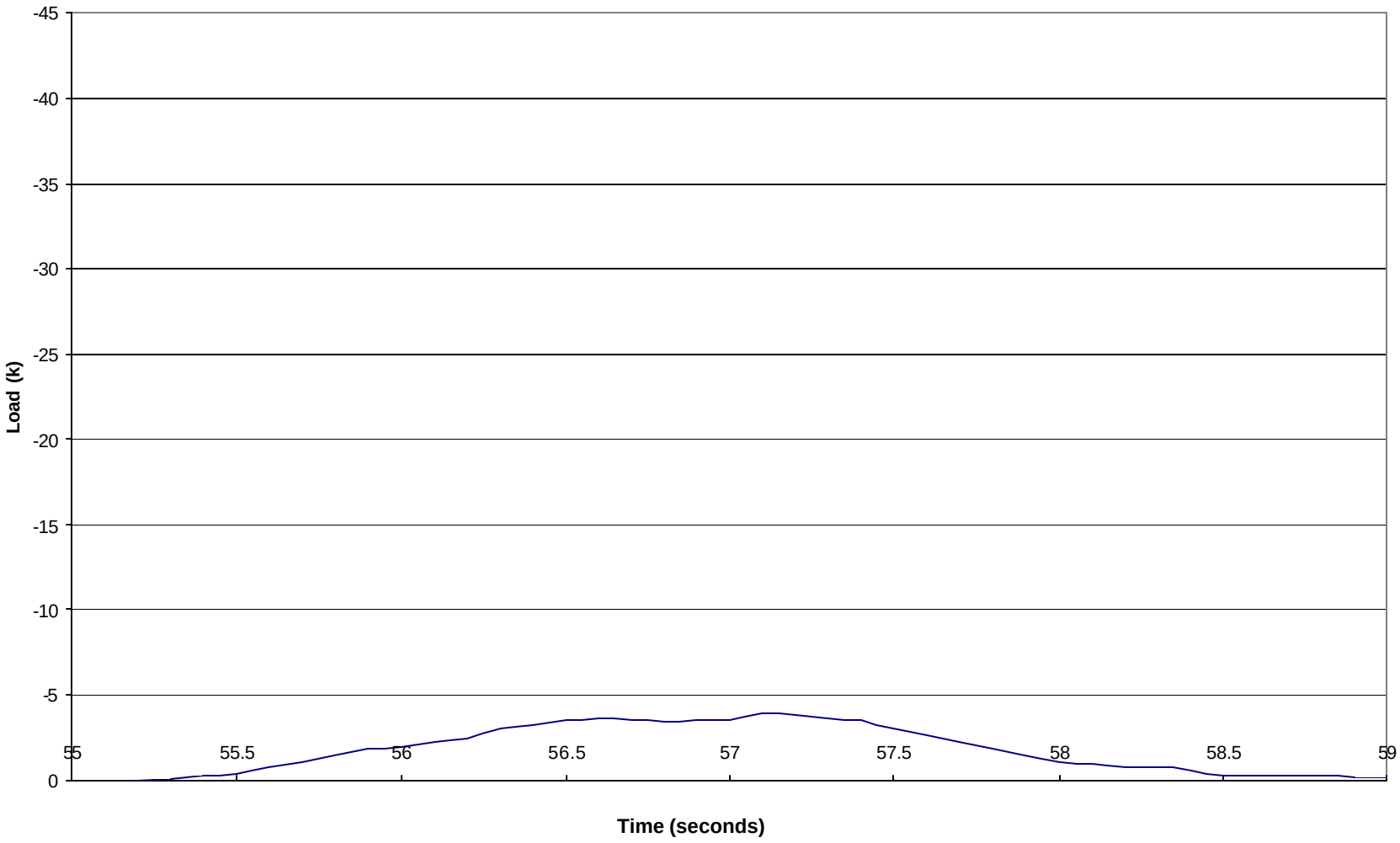

Fig. 3.1 Plot of load (Crane B) vs. time for Pile 1

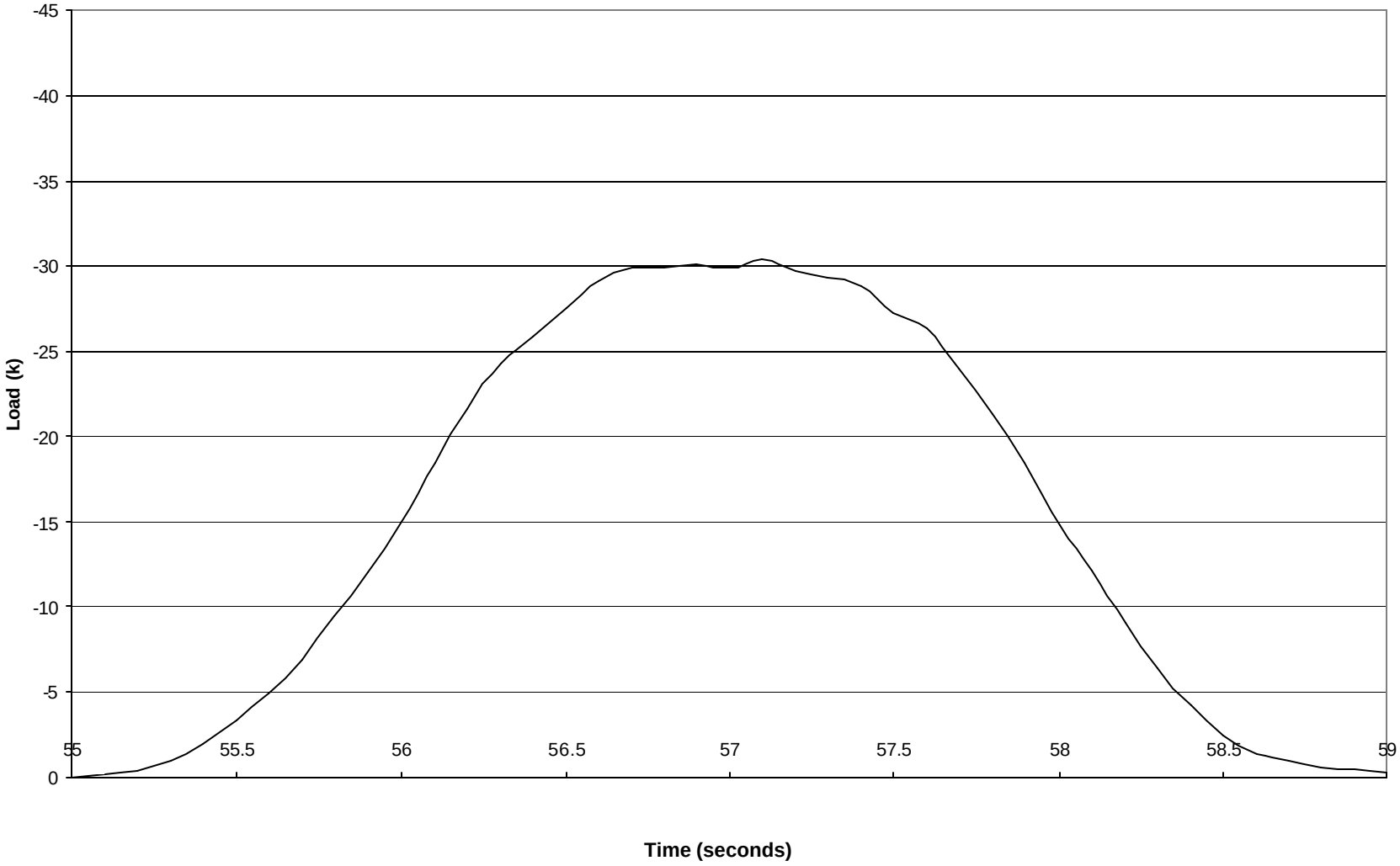

Fig. 3.2 Plot of load (Crane B) vs. time for Pile 2

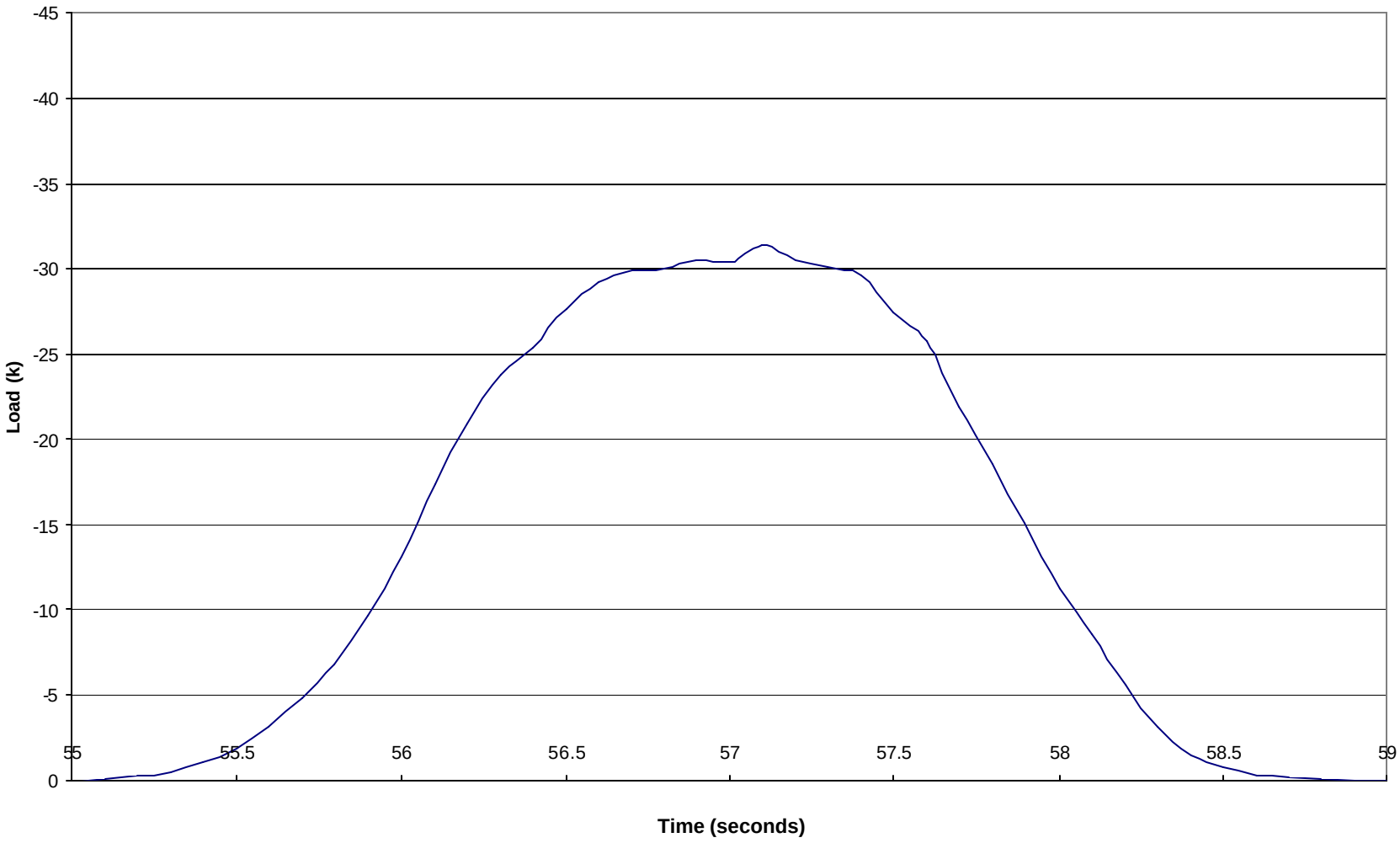

Fig. 3.3 Plot of load (Crane B) vs. time for Pile 3

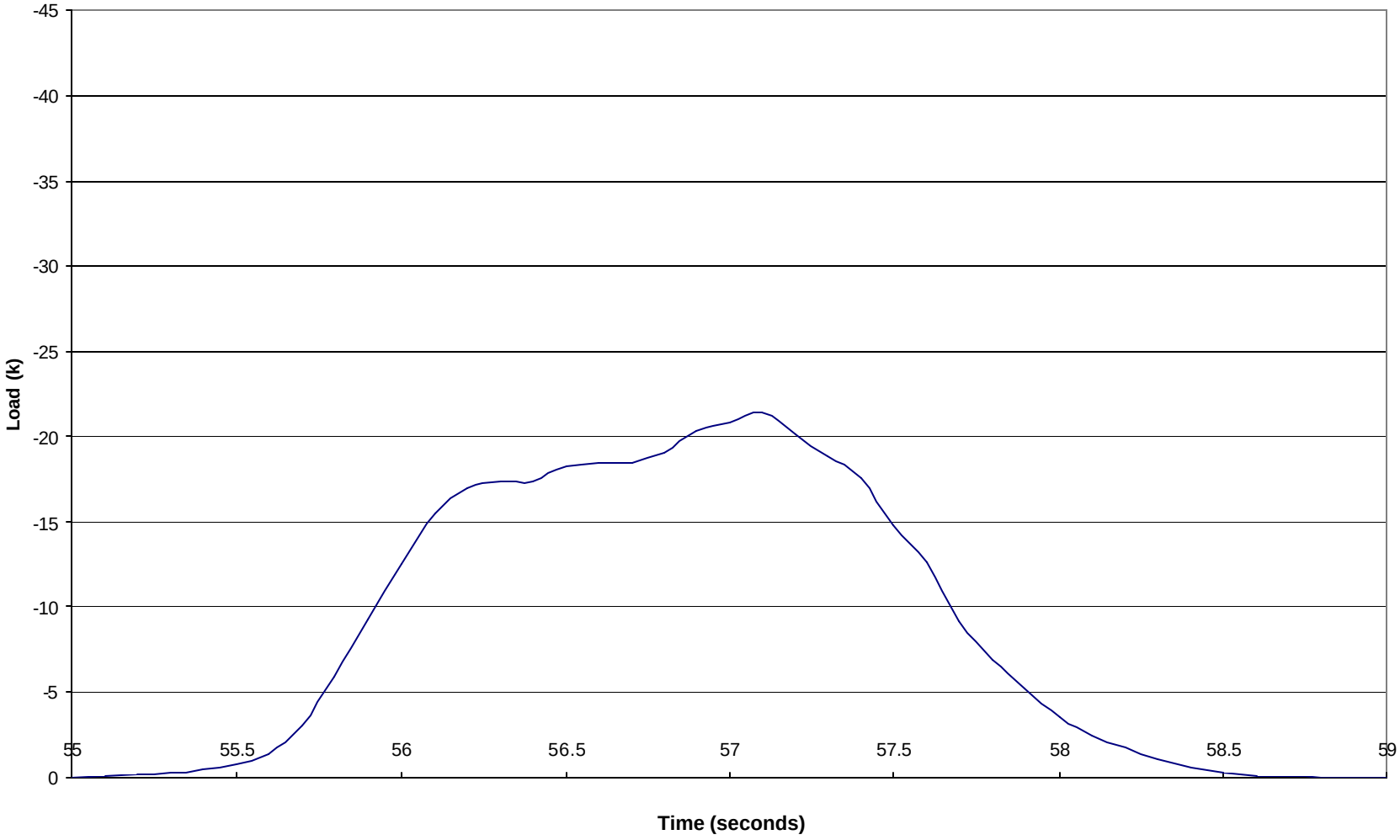

Fig. 3.4 Plot of load (Crane B) vs. time for Pile 4

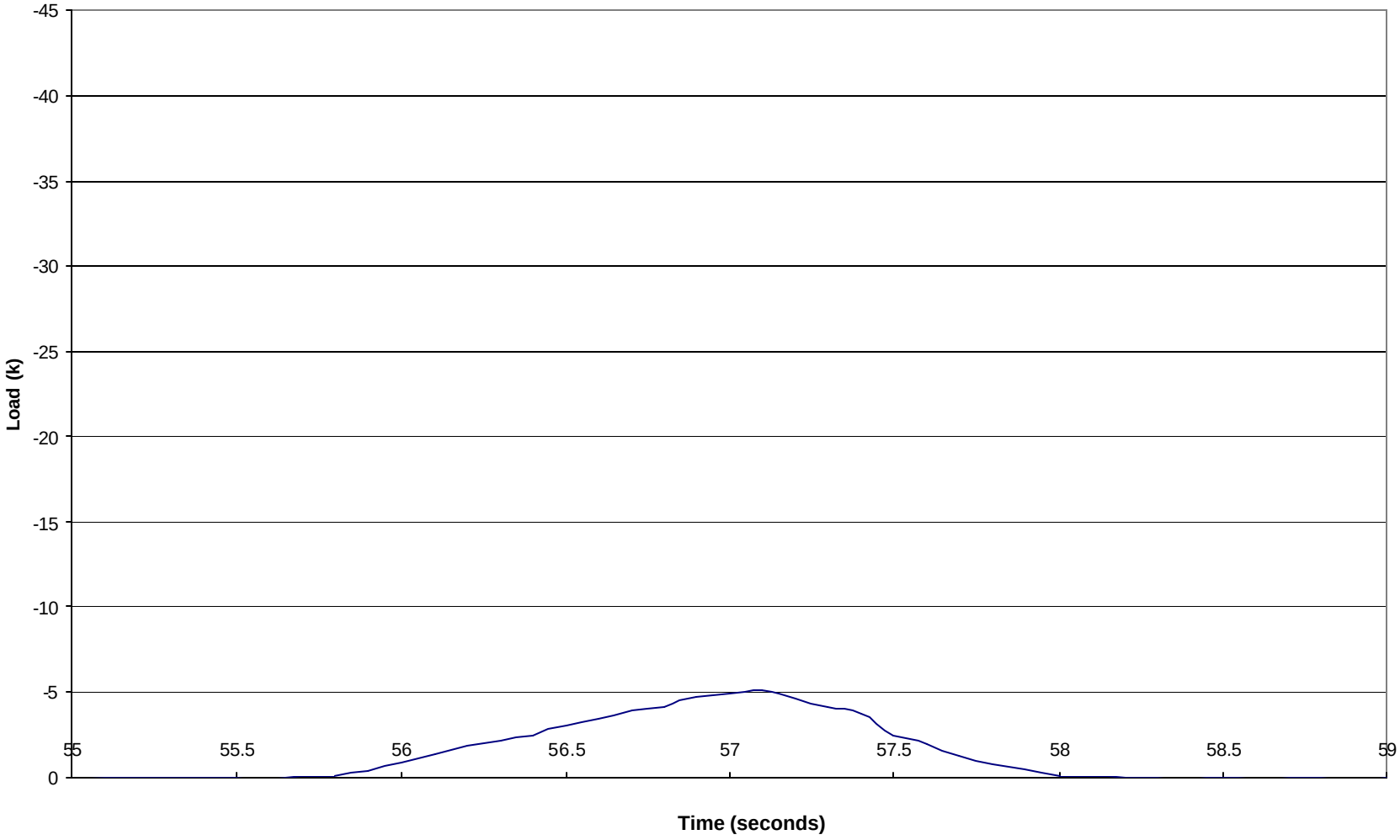

Fig. 3.5 Plot of load (Crane B) vs. time for Pile 5

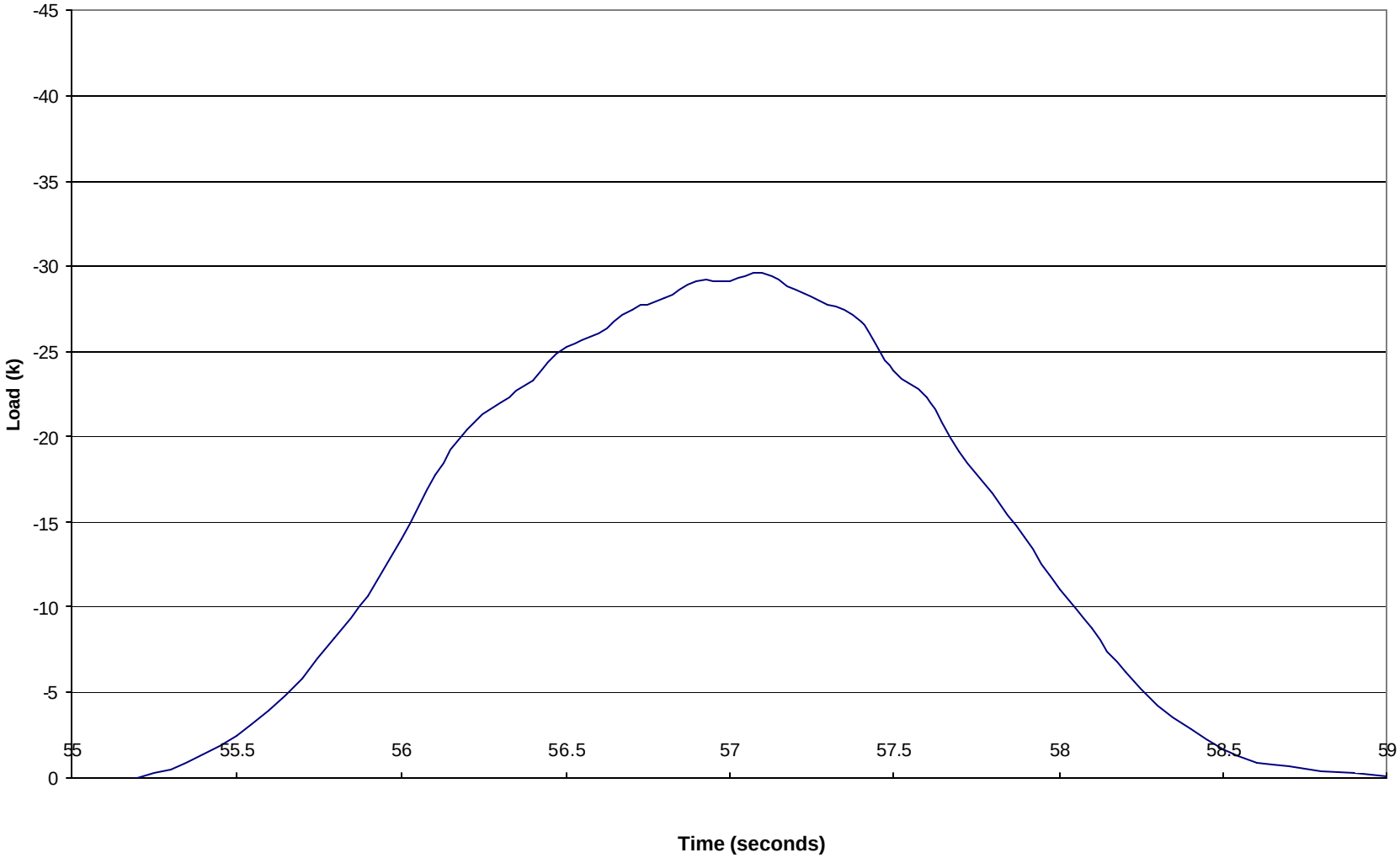

Fig. 3.6 Plot of load (Crane B) vs. time for Pile 6

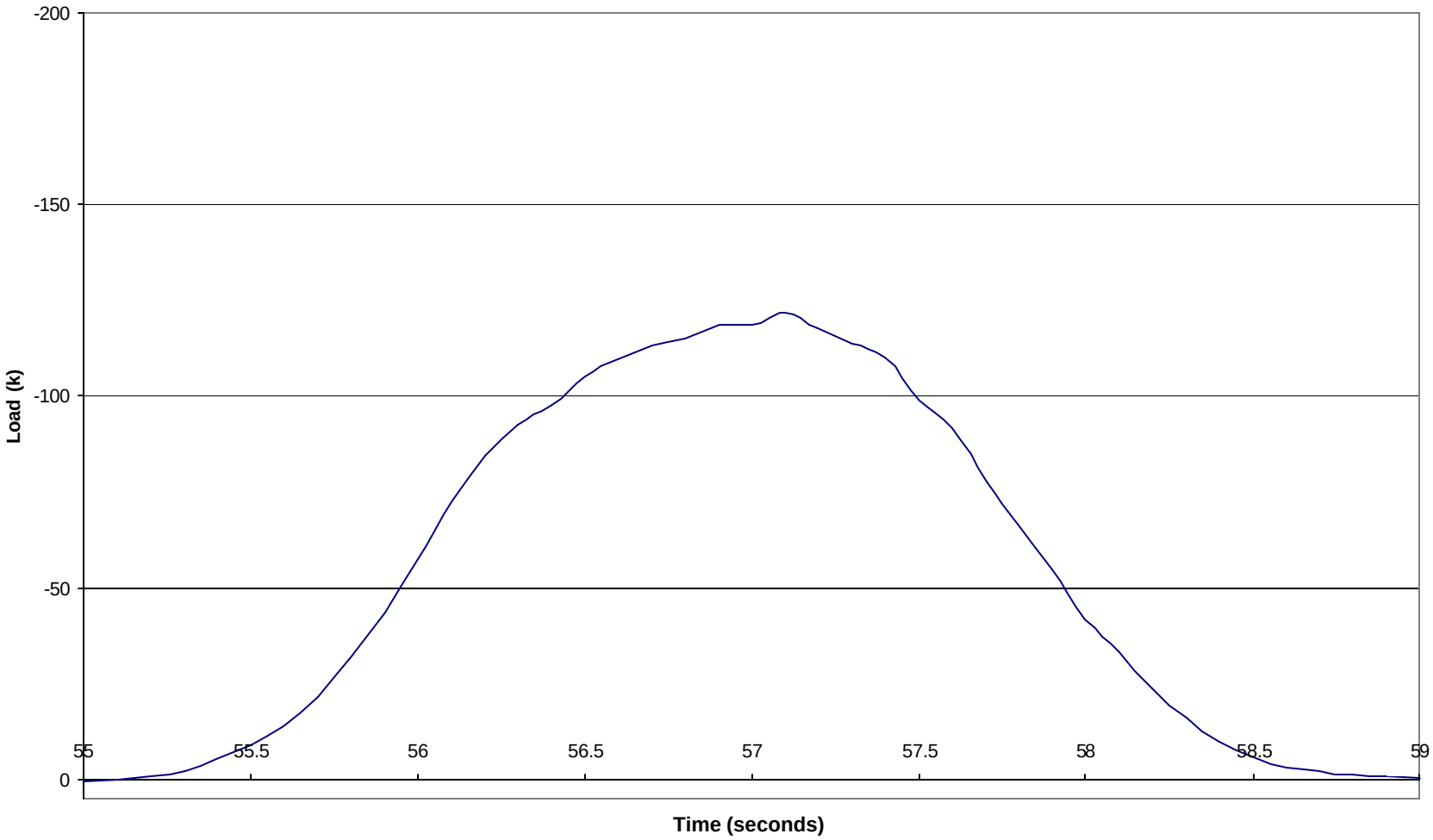

Fig. 3.7 Plot of load (Crane B) vs. time

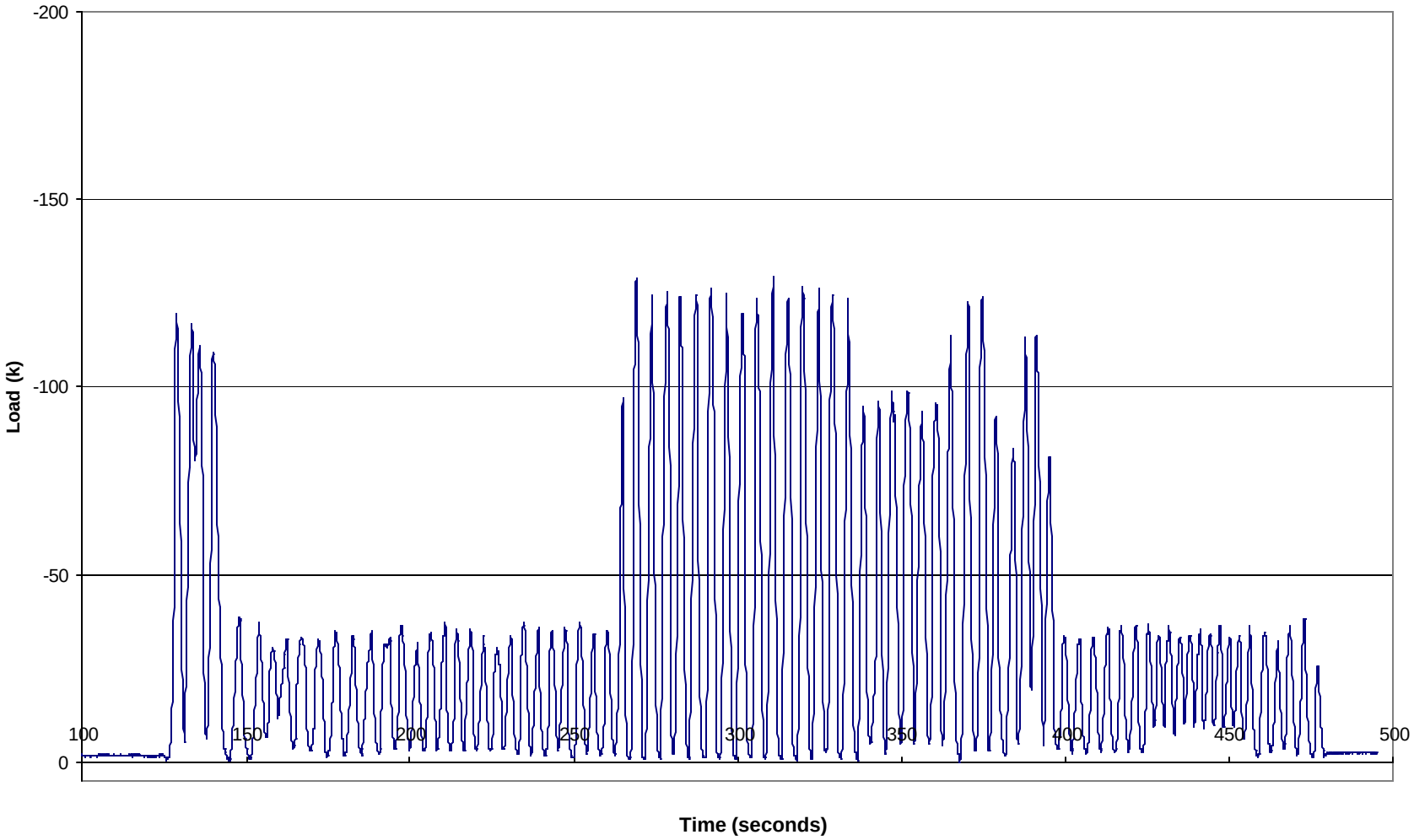

Fig. 3.8 Plot of load (Train B) vs. time

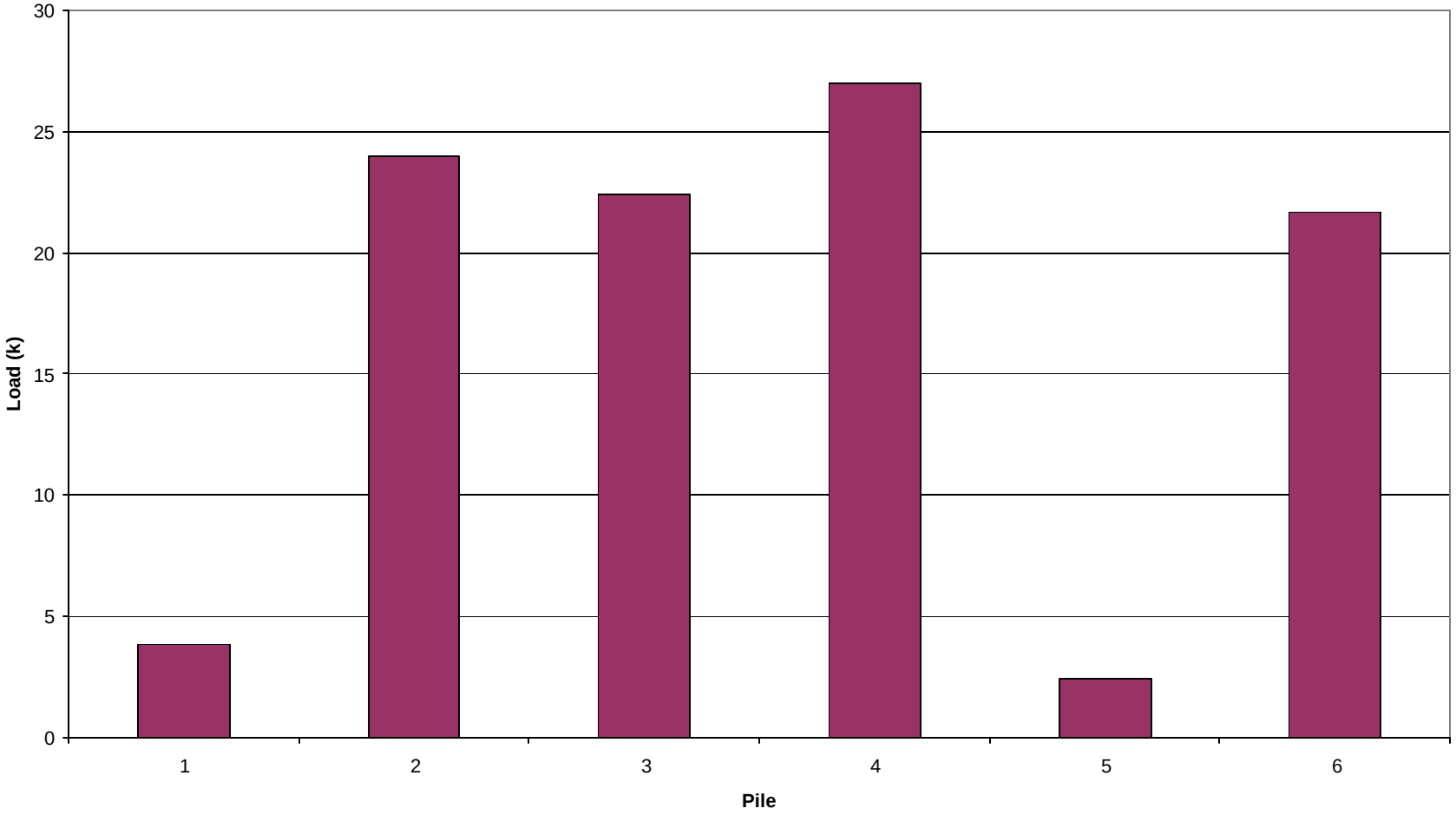

Fig. 3.9 Bar graph representing the load distribution among Piles 1 - 6

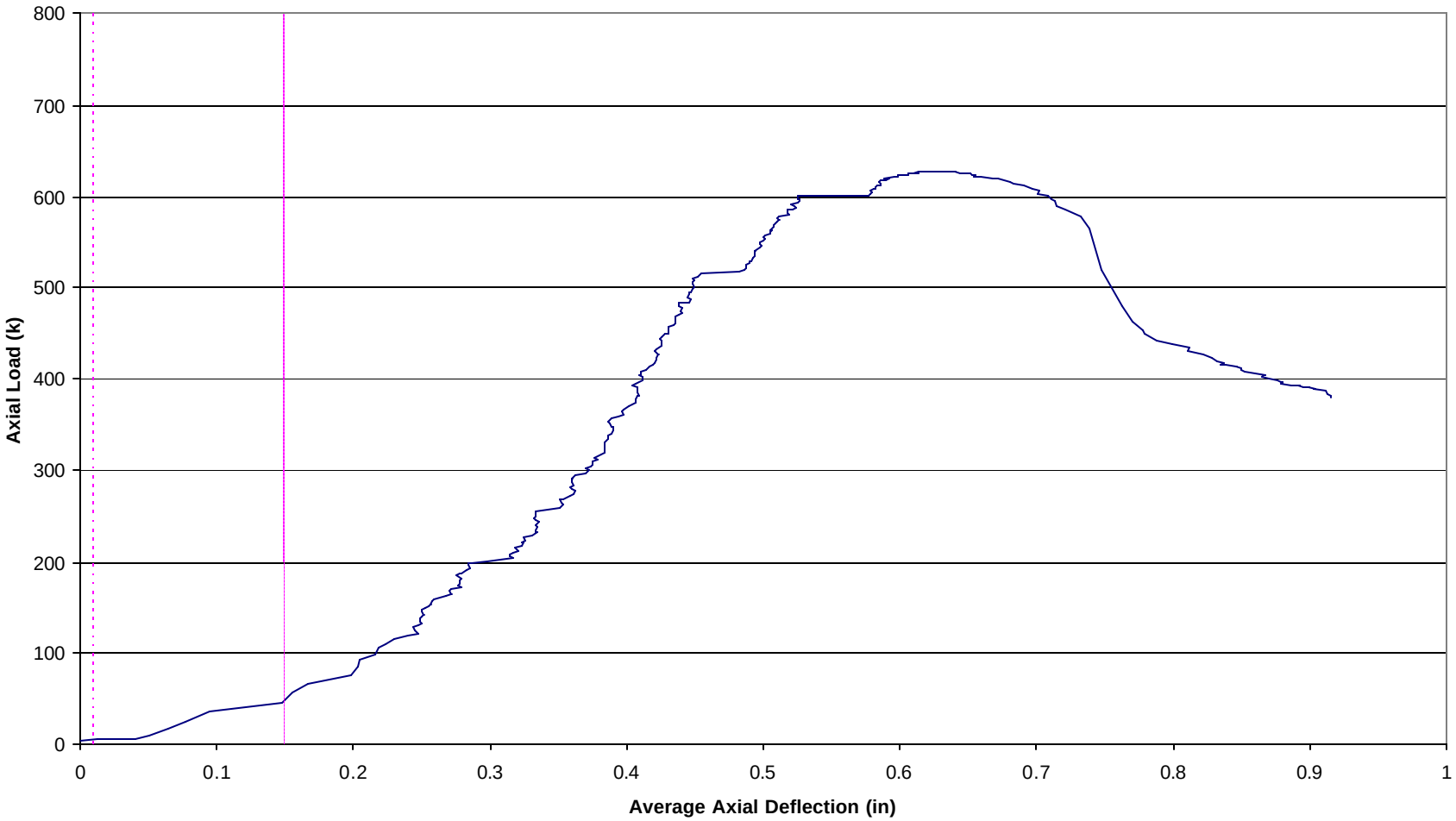

Fig. 3.10 Plot of applied load vs. average axial deflection for Pile A7 highlighting linear portion used in the derivation of strength parameter, β

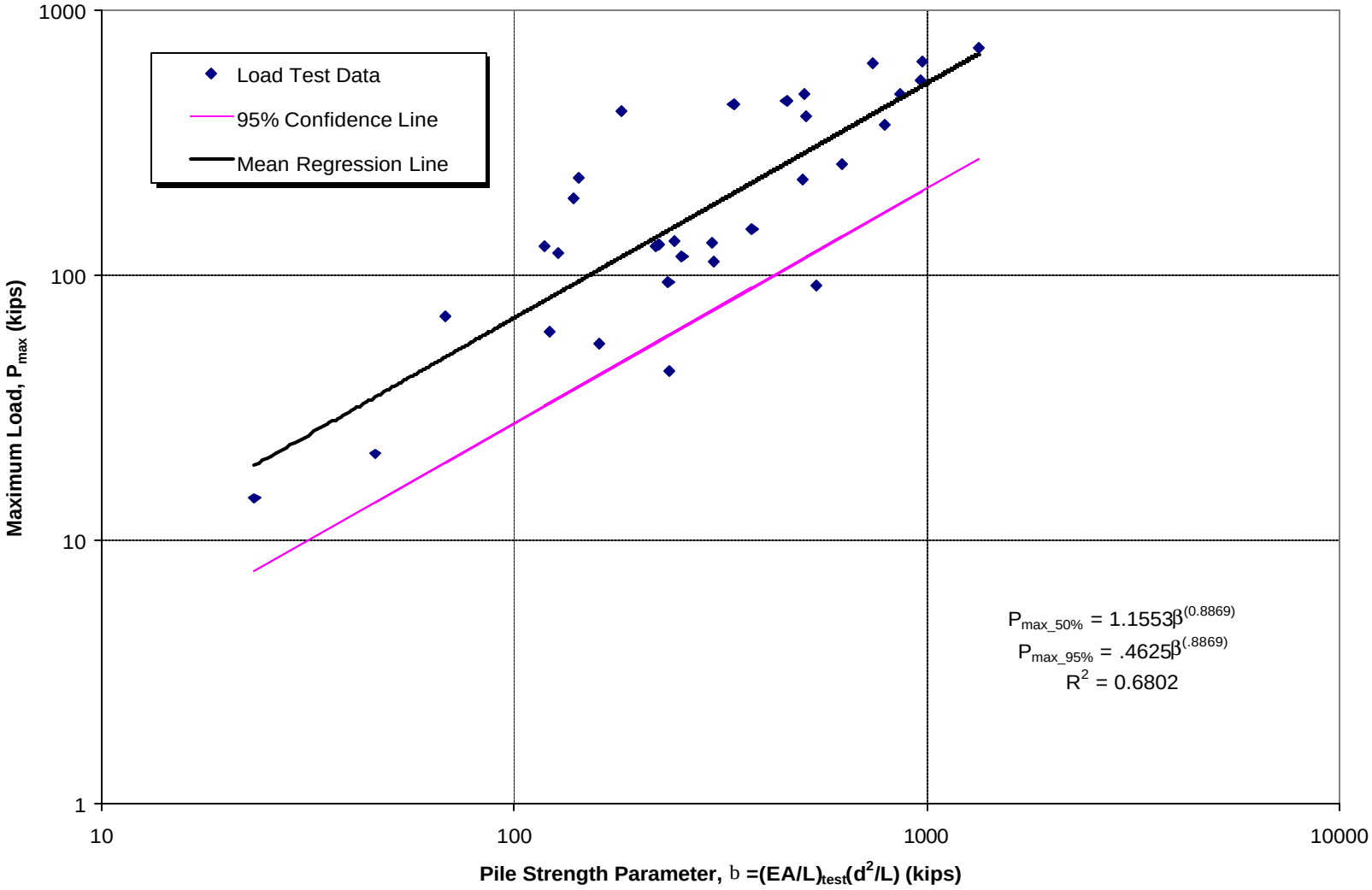

Fig. 3.11 Ultimate load vs. service pile strength parameter, β

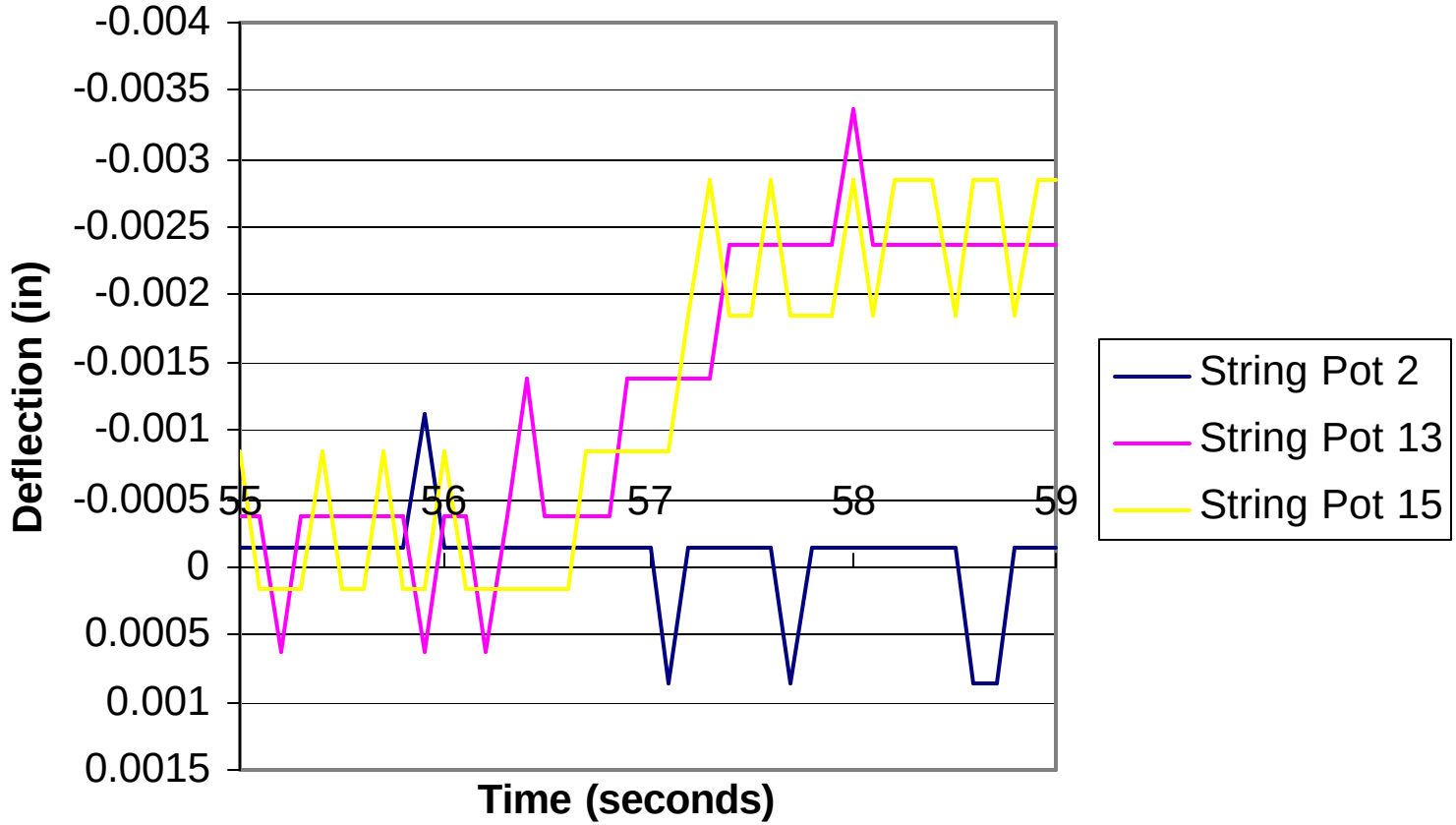

Fig. 3.12 Deflection vs. time for Pile 6 due to Crane B

APPENDIX B

TABLES

Table 1.1 Calculation of pile strength parameters for all timber piles included in the least squares regression in previous tests

Specimen Number	Length (in)	Tip Diameter (in)	L/d	P_{max} (k)	D_{max} (in)	$(EA/L)_{test}$ (for l) (k/in)	$(EA/L)_{test}$ (for b) (k/in)	l (k)	b (k)
A1	86.13	13.69	6.29	455.20	0.770	1167	209.8	2540.0	456.5
A2	96.13	12.45	7.72	416.56	0.466	1917	112	3093.0	180.6
A3	95.38	13.05	7.31	442.69	0.766	1092	189	1950.0	337.5
A4	83.80	15.52	5.40	641.78	0.466	2121	339	6093.0	974.4
A5	96.75	14.48	6.68	479.43	0.360	2291	397	4969.0	860.4
A6	79.92	11.78	6.78	398.13	0.578	1385	293	2403.0	508.7
A7	95.00	14.32	6.63	629.70	0.633	1750	343	3780.0	740.4
A8	98.38	13.85	7.10	544.62	0.403	1836	499	3578.0	973.0
A10	83.38	14.88	5.60	718.02	0.605	2180	500	5788.0	1327.8
A11	77.92	13.37	5.83	368.35	0.641	643	343	1475.0	786.9
A12	96.75	13.93	6.95	477.97	0.580	1551	252	3109.0	505.4
B2	189.50	12.89	14.70	128.00	0.345	840	252	736.0	221.0
B3	190.00	12.97	14.65	94.45	0.373	421	266	372.0	235.5
B4	193.00	13.49	14.31	128.90	0.660	254	126	239.0	118.8
C1	159.50	12.57	12.69	43.50	0.185	240	238	238.0	235.8
C2	137.00	7.56	18.12	21.05	0.079	166	109	69.0	45.5
C3	144.00	13.61	10.58	149.00	0.438	421	294	541.0	378.2
C4	147.50	12.73	11.59	134.10	0.347	466	223	512.0	245.0
C5	136.00	12.41	10.96	54.60	0.316	127	142	143.0	160.8
C6	148.00	12.57	11.77	120.90	0.481	366	119	391.0	127.0
C7	126.00	13.69	9.20	132.30	0.687	347	203	516.0	301.9
C8	159.25	13.60	11.71	61.30	0.608	97	105	112.0	122.0
C9	149.00	13.05	11.42	229.80	0.364	1048	433	1198.0	494.9
C11	152.50	13.37	11.41	231.80	0.719	553	122	648.0	143.0
C12	122.50	8.00	15.31	14.30	0.884	47	45	24.3	23.5
C14	140.50	13.85	10.14	130.50	0.387	527	165	719.0	225.3
C15	147.00	12.97	11.33	117.00	0.464	289	222	330.0	254.0
C16	178.50	13.21	13.51	194.10	0.937	233	143	227.0	139.8
C17	154.00	14.48	10.64	90.50	0.177	714	395	972.0	537.8
C18	151.50	13.21	11.47	262.50	0.968	519	543	597.0	625.5
C19	131.50	10.35	12.71	84.20	0.097	630	3957	394.0	3223.5
C20	137.50	12.89	10.67	111.70	0.275	557	251	674.0	303.3
C21	128.00	8.91	14.37	70.00	0.492	174	110	108.0	68.2

Table 3.1 Strength capacity estimates for Crane B loading

Pile	Load Case	Length (in)	Diameter (in)	(EA/L)test	b	Pmax_95% (k)
1	Crane B	83	14.30	86.95	214.22	53.98
2	Crane B	109	13.70	313.40	539.65	122.50
3	Crane B	115	10.19	Insufficient Data		
4	Crane B	109	11.14	106.70	121.48	32.64
5	Crane B	99	15.23	119.00	278.81	68.20
6	Crane B	109	13.00	Insufficient Data		

VITA

Kendra Ann Donovan was born December 6, 1980 in Houston, Texas. She graduated from William P. Clements High School in Sugar Land, Texas in 1999. She began her collegiate career at Texas A&M University, College Station, Texas in the fall of 1999. She completed her B.S. in Civil Engineering with a structural emphasis in May of 2003 with a 3.529 cumulative GPR, and in this time, she received a grant from the Undergraduate Student Research Program. The continued work on this research project throughout graduate school has been a benchmark in her obtaining a M.S. in Civil Engineering in December 2004.

Ms. Donovan can be reached at:

Kendra A. Donovan
c/o Jenee Donovan
4718 Dunleigh Ct.
Sugar Land, TX 77479